Landmarks in Earth Reinforcement, Ochiai et al. (eds),
© 2001 Swets & Zeitlinger, ISBN 90 2651 863 3

Dynamic behavior of multi-anchored reinforced soil wall in large-scale shear box

M. Futaki
B.R.I. Ministry of Land, Infrastructure and Transport, Japan

N. Aoyama
P.W.R.I. Ministry of Land, Infrastructure and Transport, Japan

K. Misawa & T. Konami
Okasan Livic Co., Ltd., Japan

M. Sato, T. Tatsui & K. Mikami
Techno-sol Co., Ltd., Japan

ABSTRACT: Based on a lot of achievement, the excellent stability of reinforced wall during the earthquake has been suggested. On the other hand, it is important to confirm the performance when a soil structure is designed. Actual size vibration test with large scale shear box was done to research the dynamic behavior of the "Multi-Anchored Reinforced Wall(MARW)". The acceleration of each part, the tension of the reinforcement material, the vertical load of the wall and the amount of deformation were measured at MARW of the height 5m during the vibration. According to the test results, following dynamic behavior of MARW were confirmed. 1)A reinforced field is unified action. 2)Increase in tension of reinforcement(Tie-bar) during the vibration is big in the connection point of the Tie-bar and the wall. 3)Increase in tension of Tie-bar during the vibration is as big as it is deep. 4)Increase in vertical load of reinforced field is big around the toe. 5)Residual stress and deformation after acceleration over 400gal are extremely small.

1 INTRODUCTION

Many retaining walls which were designed to withstand earth pressures by self-weight were severely damaged in the Hyogoken-Nanbu Earthquake in 1995. On the other hand, damage to retaining walls made of reinforced soil was light, which indicates that walls of this type have a high seismic resistance(The Japanese Geotechnical Society 1996, Kobayashi,K., Tanabe,H. and Boyd,M. 1996, Nishimura,J., Hirai,T., Iwasaki,K. et al. 1996). Although many tests using small specimens to investigate the seismic resistance of reinforced soil retaining walls have been carried out so far (Matsuo,O., Tsutsumi,T. and Saito,Y. 1999), the number of studies using full-scale specimens(Tateyama,M., Murata,O. and Tatsuoka,F. 1990) is not many. Particularly, although reinforced soil retaining walls with multi-layer anchor have been proved to be stable even during actual earthquakes, their stability mechanism has not been fully revealed.

In this study, tests using a large-scale shear box and a vibrating table were carried out to investigate earth pressures acting on a reinforced soil wall with multi-layer anchor; stresses imposed on reinforcement materials; contact pressures at the bottom of backfill area; and the deformation behaviors of the front panel during earthquakes. Furthermore, dynamic responses of a tall reinforced soil retaining wall with multi-layer anchor were analyzed to obtain data to establish a rational design method.

2 TEST APPARATUS AND TEST METHOD

The large-scale shear box in shown Fig.1 can produce simple shear deformation. The shear box is 3.6m wide, 10m long, 5m high, and it has the multi story structure that piled up 17 square frames of H-steels of 300mm×200mm. The table is vibrated with hydraulic actuators capable of giving a maximum vibration velocity of 20 kine, total weight of 4.4 MN, and amplitude of ±100mm. A separate displacement is to occur between the two adjacent frames smoothly, and many rollers work to achieve it.

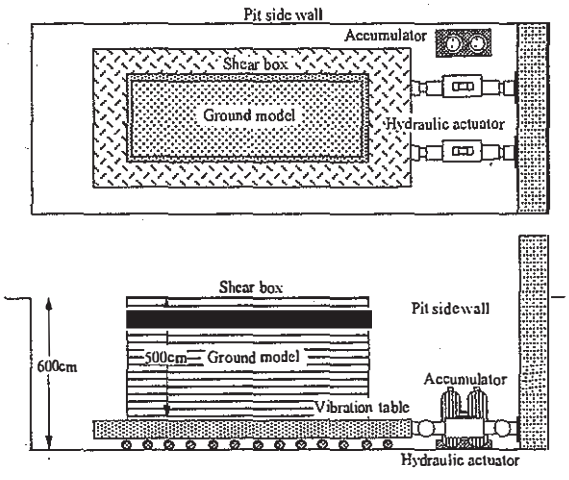

Figure 1. Schema of large-scale shear box

As shown in Fig.2, a full-scale reinforced soil retaining wall specimen measuring 5.0 m high, 3.6 m wide, and 9.0 m long was constructed in the shear box. The 3.5 m long tie bars for the reinforced area were placed 0.6 m from the active failure surface which is derived from the conventional design method, to simplify the preparation of models for dynamic response analysis and numerical simulation.

Measurement devices were placed in such a way that the ratio of forces shared by the panel and reinforcement materials and the behaviors related to bed soil stability during earthquakes (such as contact pressures) are correctly evaluated. Measurement items included horizontal and vertical forces at the bottom of the panel; distribution of contact pressures at the bottom of backfill area (measured with earth pressure cell); tension in the tie bars; response acceleration of the panel, reinforced area, backfill area behind the reinforced area, and vibration table; deformation of the shear box and ground surface; and the location of potential active failure surface (measured with strip-type tension meters).

In order to investigate the relationship between the behaviors of a reinforced soil retaining wall during earthquakes and the wall height, sweep vibration tests and step vibration tests were carried out for three different backfill heights: 3.0 m, 4.0 m, and 5.0 m. In the step vibration tests, the amplitudes of input waves were increased in stages: sine waves and actual earthquake waves (TAFT EW) were used as the input waves. The maximum response acceleration at the ground surface, obtained under these conditions, was as large as 420 gal.

3 BACKFILL MATERIAL AND BACKFILL METHOD

Nikko Silica Sand No. 6 was used as the backfill material. With a fine fraction content of 7%, a mean particle diameter of 0.25 mm, and a uniformity coefficient of 2.3, this material is classified as sand with fine fractions {S-F}. The physical and mechanical characteristics of this material are shown in Table-1. After uniformly spreading in layers with a thickness of 50 cm, the backfill material was compacted to a designated density using a small vibratory tamper. The density of the backfill material was controlled by measuring each layer's density by the core cutter method and by measuring each layer's uniformity by the dynamic plate loading tests. After the completion of backfilling, the Swedish sounding test and dynamic penetration test were conducted to check the strength of the backfill material.

The average degree of compaction of the backfill material was about 83%, which is close to the lower limit of the compaction control criterion (Dc≧85%) for this type of reinforced soil. In addition, the variation in density is relatively small.

Table-1. Physical and mechanical characteristics.

Item	Value	備 考
Soil particle density ρ_s g/cm³	2.670	
Maximum dry density ρ_{dmax} g/cm³	1.698	
Minimum dry density ρ_{dmin} g/cm³	1.326	
Maximum grain size mm	0.85	
Gravel fraction 2～75mm %	0	Sand include fine fraction {S-F}
Sand fraction 75μm～2mm %	93	
Fine fraction <75μm %	7	
Coefficient of uniformity Uc	2.34	
Cohesion c' kN/m²	0	Dc=83% Triaxial test(CU)
Internal friction angle φ' degree	32.8	

4 TEST RESULTS

4.1 *Frequency characteristics*

The results of sweep vibration tests are shown in Fig. 3: the left diagram gives the ratio between the response acceleration spectrum at the ground surface of the front section of the reinforced area and accelcration spectrum of the vibration table, while the right diagram shows the ratio between the response acceleration spectrum at the ground surface of four areas (wall height: 5 m) and the acceleration spectrum of the vibration table. The resonance frequency of a specimen with a wall height of 3.0 m, 4.0 m, and 5.0 m was 7.5 Hz, 5.5 Hz, and 4.5 Hz, respectively. This means that the more higher the wall (therefore the heavier), the smaller the resonance

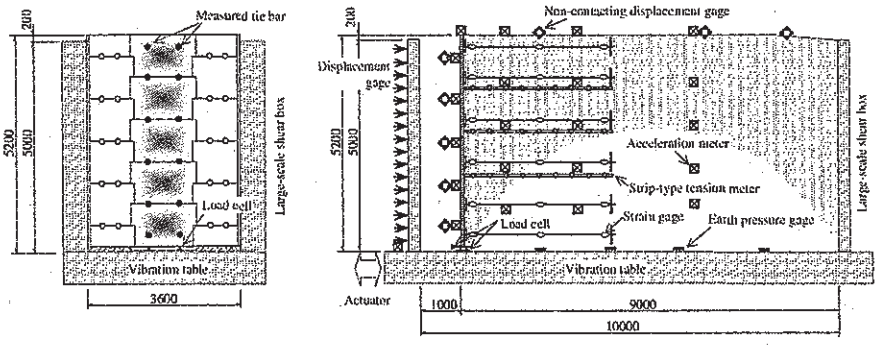

Figure 2. Full-scale reinforced soil retaining wall specimen.

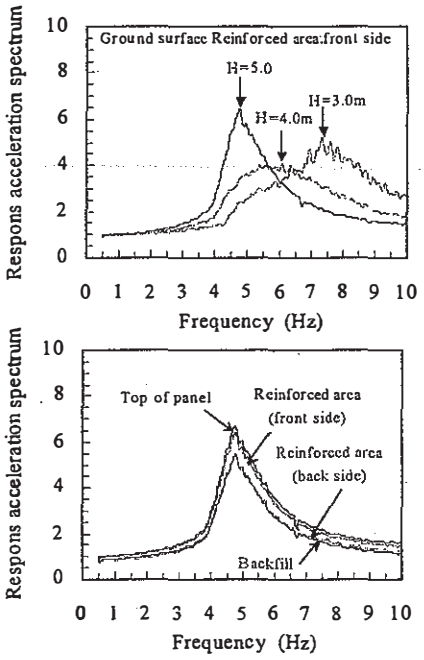

Figure 3. Results of sweep vibration tests.

frequency. The responses of ground surfaces (within reinforced area), the front panel, and the backfill area behind the reinforced area to the vibration of the table are almost the same, which indicates that the reinforced area and the backfill material behind it behaves like a composite mass.

4.2 *Response acceleration characteristics*

Fig.4 shows the response acceleration of the panel, reinforced area, and backfill area behind the reinforced area during vibration. Although there are some variation depending on the magnitude of the input acceleration, the accelerations at the ground surface level of the front panel, reinforced area, and backfill area behind the reinforced area have a phase difference to the vibration table's acceleration of between $\pi/4$ to $2/3\pi$. However, the behavior in which reinforced area and backfill area were almost united is proven on response acceleration in each these

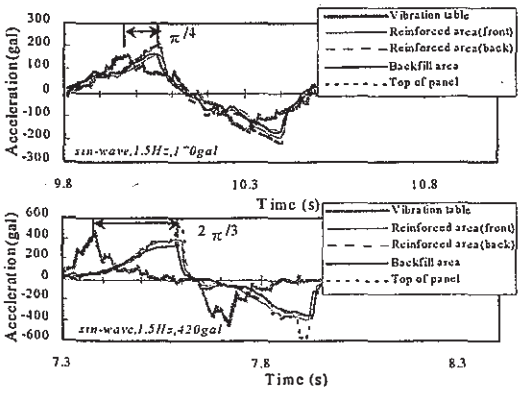

Figure 4. Response acceleration during vibration.

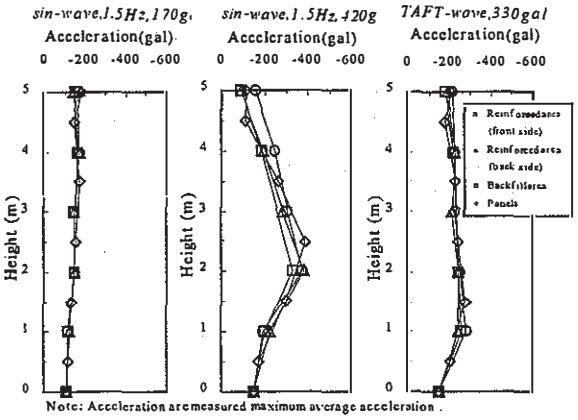

Figure 5. Distribution of response acceleration.

place surface, because the almost equal response characteristic is shown. Fig.5 shows the distribution of response acceleration of the front panel, reinforced area and the backfill area behind the reinforced area. This figure also indicates that the front panel, reinforced area, and backfill area behind the reinforced area behave like a composite mass, since their response accelerations have similar profile. However, the shape and magnitude of the curve for response acceleration change depending on the maximum acceleration and shape of input ground motion.

4.3 *Actual tension in tie bars*

Strain gauges were placed on the surface of steel tie bars to measure the tension (corresponding to earth pressures acting on the panel surface) imposed on them and verify the magnitude and distributions of forces acting on the front panel which occur during vibration. Fig.6 shows the relationship of the depth with the tensile forces in tie bars during vibration and with the maximum tension(increment) at the time of the maximum average acceleration. Since the tension given in this figure were measured near the panel, they are considered to be close to the earth pressures. As shown in this figure, the tensile and

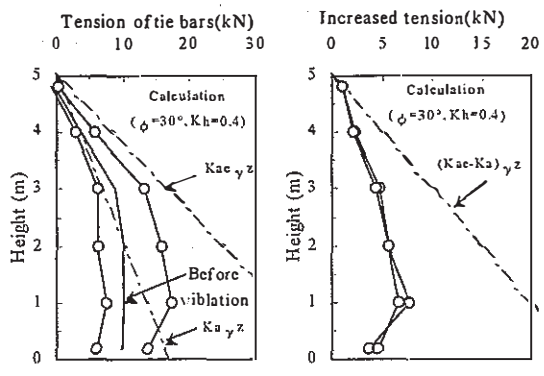

Figure 6. Maximum increment tension of tie bars.

compressive forces in tie bars during vibration are caused by active and passive earth pressures, with tension dominant, and the directions of the forces are the same regardless of the depths. In addition, the maximum increment of the tension in tie bars is nearly proportional to the depth, but smaller than the values calculated using the current design method. In addition, as shown in Fig.7, the increment of tension in tie bars during vibration is small near the anchor plate due to the surface friction of the bars, but large near the panel.

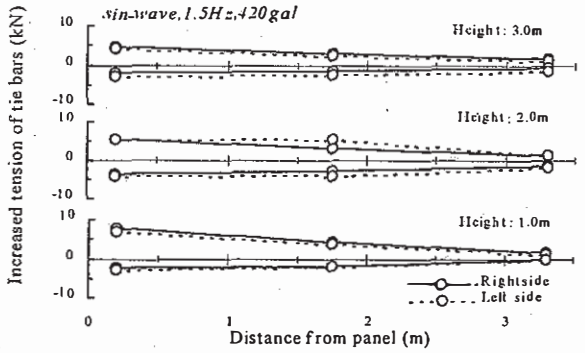

Figure 7. Distribution of increment tension of tie bars.

4.4 *Contact pressures at the bottom of the backfill*

In order to obtain information for checking the bearing capacity during earthquakes, the magnitude and distributions of the contact pressures at the bottom of both the front panel and backfill area were investigated. Fig.8 shows the distributions of the contact pressures at the bottom of the backfill area. As shown in this figure, the contact pressures working at the bottom of the backfill area during earthquakes increase and decrease from those during stationary state depending on the direction of vibration. The increase in contact pressures tends to be larger at the location immediately behind the panel than at the locations away from the panel. Contact pressures after vibration were almost the same as those during stationary conditions, and residual contact pressures due to vibration were negligible.

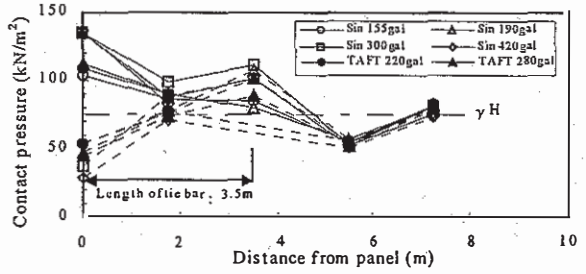

Figure 8. Distribution of contact pressure.

4.5 *Deformation behavior of the panel*

The left diagram of Fig.9 shows the distribution of panel displacement at the time of maximum average acceleration, when the input ground motion has a frequency of 1.5 Hz and an acceleration of 420 gal, while the right diagram compares the maximum displacement amplitude for input ground motions with various accelerations. The displacement distribution of the 5-m height during vibration for each input ground motion was in the primary mode. The maximum displacement at the top of the front panel was about 50 mm for a ground acceleration of about 400 gal. In addition, the residual displacement after vibration was relatively small.

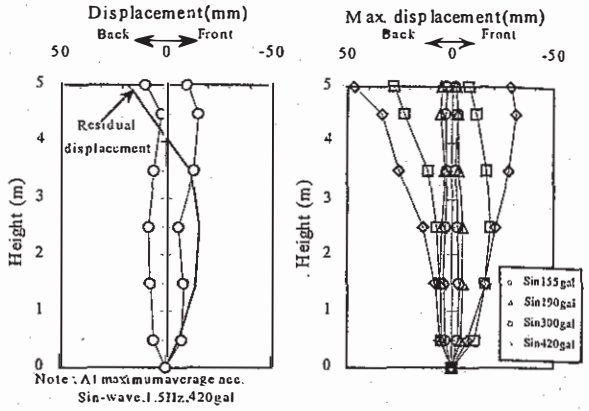

Figure 9. Distribution of panel displacement.

4.6 *Active failure surface during earthquakes*

In order to identify the location of active failure surface for both during vibration and during stationary conditions, strip type tensile meters were embedded in the reinforced area. Fig.10 shows the strains in the strips. As shown in this figure, locations for the peak

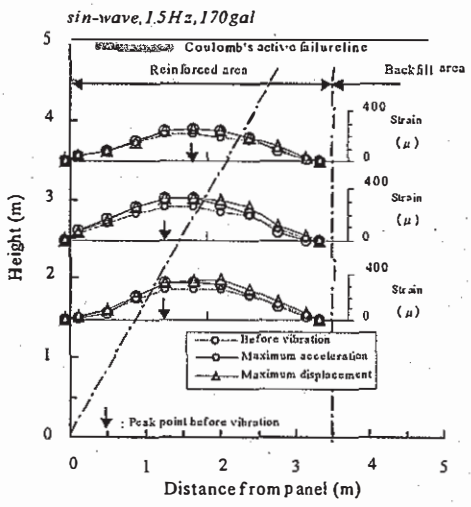

Figure 10. Strain in the strip-type tension meters.

values are almost the same. This means that the active failure surface does not move backward and the soil behind the front panel behaves like a composite mass because of the effect of the reinforcement materials.

4.7 *Ground deformation after vibration*

Fig.11 shows the locations of vibration-induced cracks in the ground behind the front panel and in the ground surface. The locations of cracks in the ground behind the front panel were identified when the role paper placed in the ground was removed. As shown in the figure, cracks are observed only in the ground behind the reinforced area. It should be noted that the cracks appear near and behind the Coulomb's active failure surface.

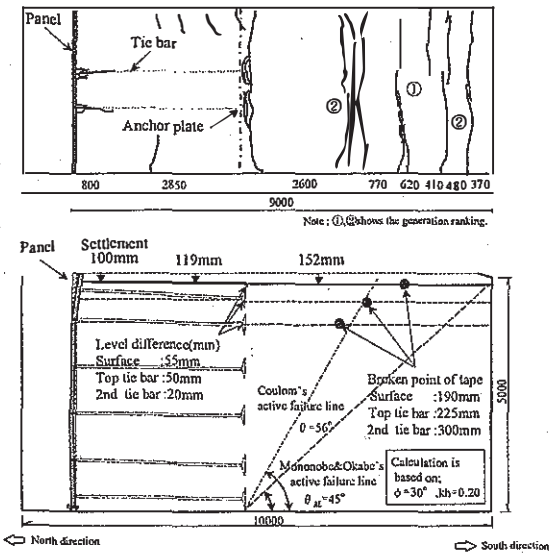

Figure 11. Cracks in the behind the panel and ground surface.

5 DYNAMIC ANALYSIS

5.1 *Method of analysis*

The analysis is called "Super FLUSH" was used as the two-dimensional plane strain condition. Finite element mesh is shown in Fig.12. This model is used 1197 joint nodes and 1120 elements. A boundary condition set up free at the bottom part, fixed at the wall, and free only the horizontal direction in shear box boundary. Moreover, backfill materials, panel materials, side-glance area materials, and anchor plates were made a plane element. Then equivalent line shape wasn't taken into consideration, and it was made elasticity. And, the mass of shear box are ignored because it is small in comparison with the backfill. Input parameters are shown in Table-2. Modulus of the backfill material is considered as confining pressure dependence using the result of soil test.

Table-2. Input parameters

Material	Unit weight (kN/m³)	Modulus of deformation (MN/m²)	Poisson ratio
Embankment	15	12.1~42.2	0.45
Wall(Panels)	26	2,100	0.20
Joint filler fee	5	5	0.10
Anchor rods	79	2,100	0.29

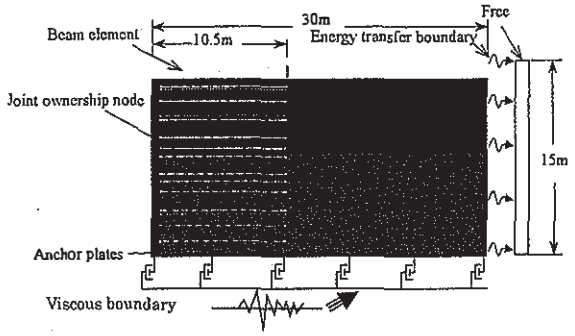

Figure 12. Finite element mesh.

5.2 *Results of simulation for the vibration test*

The depth distribution of the response acceleration at the wall which are measurement value by the shaking table test and the dynamic analytic result is shown in Fig.13. This figure shows that it can confirm that it almost corresponds as for the analytic result and the experiment value, when the input acceleration of the shaking table is small. When input acceleration is big (sin-wave 400gal), the deformation mode of the wall becomes the multiple modes, and some difference is admitted in the experiment result and the analytic result about the response acceleration of the wall. But, as for the average response acceleration in the depth direction, it is understood that it has good adjustment. The depth distribution of wall displacement got from vibration experiment and dynamic analysis is shown in Fig.14. When input acceleration is small, good correlation is presumed an experiment result and analytic result in the same way as the depth distribution of the response acceleration. But, the difference around the ground surface grows big when input acceleration grows big. And it is understood that an analytic re-

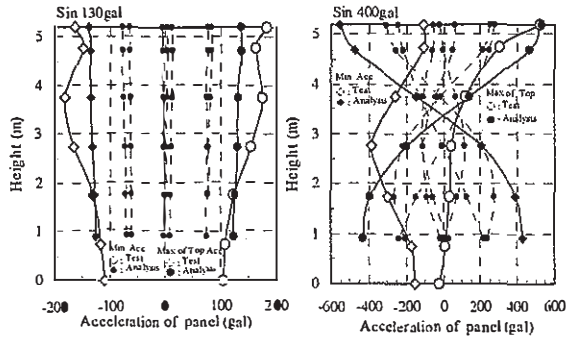

Figure 13. Distribution of response acceleration of panel.

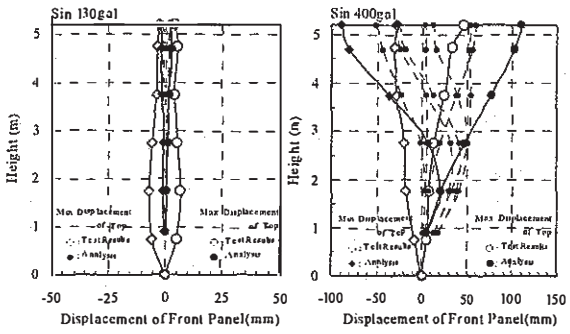

Figure 14. Distribution of response displacement of panel.

sult is beyond the measurement value. The basic performance of the analytic program was verified from these things as a result of comparing measurement value with analytic value in the deformation nature of the wall and the response acceleration. Therefore, it was judged that to simulate the behavior in of reinforced soil wall using the dynamic analysis was precisely possible.

5.3 *Results of dynamic analysis for the wall height 15m-class*

This object is valuation of the resistance to earthquake of the multi-anchored reinforced soil wall, and the dynamic analysis are done by using the verified analytic program about the wall height 15m-class. Considering large and medium-scale ground vibration level, the shape of seismic wave adopted the shaking wave which compressed maximum acceleration amplitude in the place in 150gal, 400gal (KOBE N-S direction). An example of the analytic result is shown in Fig. 15. The various modes exist in the response acceleration distribution toward input acceleration by earthquake. But, as for the acceleration inputted from the base, it is understood that it doesn't amplify in the backfill and around ground surface too much. Moreover, the deformation of the crest of panels is about 20cm during the large-scale ground vibration level, and this value is about equivalent on the displacement angle of 1.5/100. At this time, it is understood that tension of about the maximum 20kN/m^2 appears in the neighborhood of the ground surface or the bottom part in tie bars. And, contact pressure is changing about 20% to customary pressure at the foundation under the panels. The result of arranging the predictive value in each of large and medium-scale ground vibration level is shown in Table-3. Earth pressure against wall in the large-scale vibration level is the degree that it is the same as in the medium-scale, as an absolute value. However, sufficient consideration seems to be necessary, when the appearance depth reaches near the ground level, and when that the withdrawal resistance of the anchor plate is the small range is considered.

It is considered that the stability of the wall height 15m-class can be verified fully as a result examined about the stability during the earthquake of the multi-anchored reinforced soil wall by the dynamic analysis. And, it can be expected that rational design method of the multi-anchored reinforced soil wall becomes possible these result by the reflection of the seismic designing method.

Table-3. Results of analysis for 15m-height class

Earthquake Level	Response acc. magnification	Distortion angle (half-amp.)	Tension of tie bars (earth pressure)	Contact pressure (ratio)
Medium-scale	1.3	$\frac{0.4}{100}$	20kN/m^2 (bottom)	15%
Large-scale	0.9	$\frac{1.5}{100}$	20kN/m^2 (bottom, surface)	20%

6 CONCLUSION

The following findings were obtained from the vibration tests using full-scale specimens of multi-anchored reinforced soil wall:

1) The panel, reinforced area behind the panel, and the backfill area behind the reinforced area behave like a composite mass. The distributions of the response acceleration, however, vary depending on the acceleration and shape of the input waves.

2) Although the increments of the tensile forces in tie bars are generally proportional to the depth,

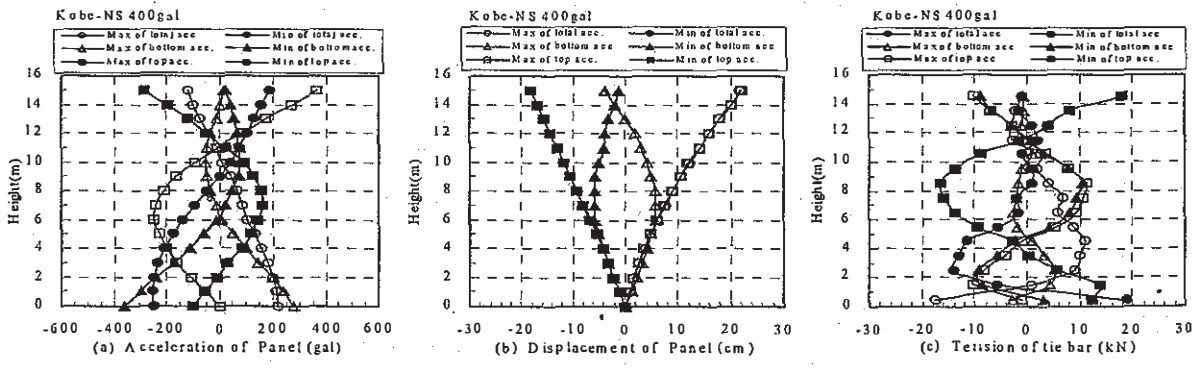

Figure 15. An example of the analytic results.

their values are smaller than those derived from the current calculation method.

3) Contact pressures at the bottom of the backfill area during vibration tend to be large at the location immediately behind the front panel. Their values after vibration, however, are almost the same as those before vibration: residual contact pressures are negligible.

4) The displacement at the top of the front panel during vibration is about 50 mm for a ground acceleration of 400 gal. The residual displacement after vibration is relatively small.

5) The active failure surface does not move backward during earthquakes. This indicates that the reinforced area forms a composite mass.

6) No cracks in the reinforced area were observed during visual inspection after vibration. Cracks were found only in the area behind the reinforced area.

7) It is considered that the stability of the wall height 15m-class can be verified fully as a result examined about the stability during the earthquake of the multi-anchored reinforced soil wall by the dynamic analysis.

REFERENCES

The Japanese Geotechnical Society 1996: *Report of damage for the Great Hanshin Awaji earthquake*, pp.327-341.

Kobayashi,K., Tanabe,H. and Boyd,M. 1996. The performance of reinforced earth structures in the vicinity of Kobe during the Great Hanshin Earthquake: *Proc. of the International symposium on earth reinforcement(IS Kyushu '96)*, pp.395-400.

Nishimura,J., Hirai,T., Iwasaki,K. et al. 1996. Earthquake resistance of geogrid-reinforced soil walls based on study conducted following the southern Hyogo earthquake: *Proc. of the International symposium on earth reinforcement(IS Kyushu '96)*, pp.439-444.

Matsuo,O., Tsutsumi,T. and Saito,Y. 1999. Shaking table tests and stability analysis on seismic performance of geosynthetic-reinforced soil retaining walls: *Civil engineering journal*, Vol.41, No.1.p.32-37.